

## Functionalization of Synthesized Nanoporous Silica and Its Application in Malachite Green Removal from Contaminated Water

Bahman Hassan-Zadeh<sup>1</sup>, Reza Rahmanian<sup>1</sup>, Mohammad Hossein Salmani<sup>2</sup>, Mohammad Javad Salmani<sup>3\*</sup>

<sup>1</sup> Department of Chemical Technology, Iranian Research and Organization for Science and Technology, Tehran, Iran.

<sup>2</sup> Environmental Science and Technology Research Center, Department of Environmental Health Engineering, School of Public Health, Shahid Sadoughi University of Medical Sciences, Yazd, Iran.

<sup>3</sup> DVM Student, Faculty of Veterinary Medicine, Shahid Bahonar University of Kerman, Kerman, Iran.

### ARTICLE INFO

#### ORIGINAL ARTICLE

#### Article History:

Received: 15 February 2021

Accepted: 20 May 2021

#### \*Corresponding Author:

Mohammad Javad Salmani

#### Email:

mjsalmani80@Yahoo.com

#### Tel:

+983531492234

#### Keywords:

Functionalization,  
Malachite Green,  
Water Pollution,  
Silicon Dioxide.

### ABSTRACT

**Introduction:** Nanoporous silica has received growing interest for its unique application potential in pollutant removal. Therefore, the development of a simple technique is required to synthesize and functionalize the nanoporous materials for industrial application.

**Materials and Methods:** The synthesis of nanoporous silica was investigated by the template sol-gel method, and it functionalized as an adsorbent for adsorption of malachite green. The morphology and structure of the prepared and functionalized nanoporous silica were studied using X-ray diffraction, Fourier transform infrared spectroscopy (FT-IR), and nitrogen adsorption-desorption technique. Subsequently, the effective parameters such as solution pH, contact time, and initial concentration on the adsorption process were optimized by adsorption tests.

**Results:** The results showed that high-order nanoporous silica had been produced with an average diameter of 20.12 nm and average pore volume of 1.04 cm<sup>3</sup>.g<sup>-1</sup>. It was found that the optimum parameters of pH, initial concentration and contact time for malachite green adsorption on nanoporous silica were 6.5, 10 mg.l<sup>-1</sup> and 60 min, respectively. The experimental data confirmed the Freundlich model (R<sup>2</sup> = 0.995) and the obtained kinetic data followed the pseudo-first-order equation. The maximum adsorption capacity calculated by Langmuir isotherm was found to be 116.3 mg.g<sup>-1</sup>.

**Conclusion:** The high adsorption capacity showed that the acid-functionalized nanoporous silica adsorbent can be used as an adequate adsorbent to remove malachite green from aquatic environments. The large surface area can be suggested that the silica nanoporous will have potential application prospects as the adsorbent.

**Citation:** Hassan-Zadeh B, Rahmanian R, Salmani MH, et al. *Functionalization of synthesized nanoporous silica and its application in Malachite Green removal from contaminated water*. J Environ Health Sustain Dev. 2021; 6(2): 1311-20.

### Introduction

Porous materials are classified into three kinds: microporous (pore diameter less than 2 nm), mesoporous (pore diameters between 2 and 50 nm), and macroporous (pore diameters greater than 50 nm). The term nanoporous is applied for those porous materials with a diameter less than

100 nm. Porous solids, particularly nanoporous materials, are generally used as adsorbents, catalysts, and catalytic bases due to having a higher surface area<sup>1, 2</sup>. Among these, the MCM-41, SAB-15, and HMS are some of the mesoporous materials with the ordered pore structures as certain forms (hexagonal-cylinder)

widely used in catalytic processes<sup>3</sup>. The SBA-type silica materials are usually synthesized in the presence of nonionic surfactants. These substances synthesized by the interaction of  $\text{EO}_x\text{PO}_y\text{EO}_x$  block copolymer with silica minerals via hydrogen bonding are carried out under acidic conditions<sup>4</sup>. The production is shown as  $\text{S}^0(\text{XI})^0$ , where S is a surfactant with the zero electric

charges, I is mineral species, and x is a negative charge ion. Figure 1a illustrates the interaction of surfactant and the silica source in the presence of the ion-pair ( $\text{H}^+$  and  $\text{Cl}^-$ ). Figure 1b shows the structure of mesoporous SBA-15 and the hexagonal arrangement of its cavities, as well as the connection mode of major canals as to small lateral canals<sup>5</sup>.

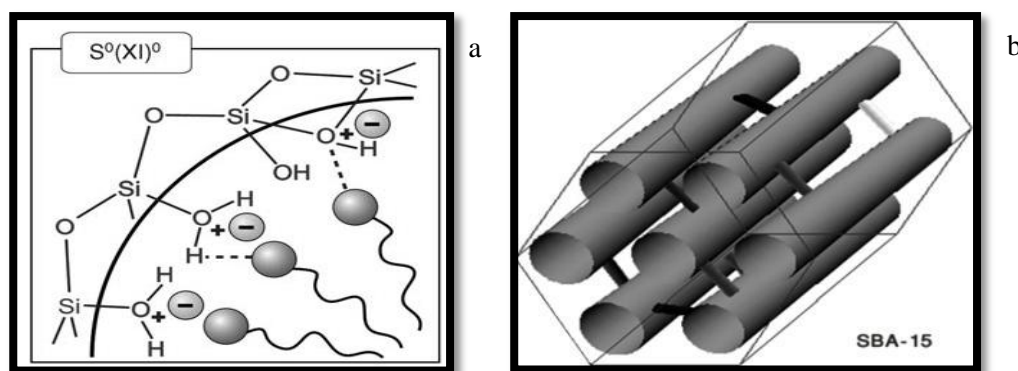


**Figure 1:** a) Interaction of surfactant and silica source b) the structure of mesoporous SBA-15

The most common methods for removing organic pollutants from wastewater are catalytic oxidation, photocatalytic oxidation, coagulation, and adsorption using activated carbon, inexpensive adsorbents, and nano adsorbents<sup>6-8</sup>. Among these methods, adsorption is regarded as a stable separation process and an effective manner for aquatic depollution. Low cost, high flexibility, easy design and composition, and high sensitivity to toxic substances in water purification and treatment make it surpass the other techniques. Moreover, it does not produce dangerous by products<sup>9,10</sup>. The key point in the removal of dyes using adsorbents is the providing of efficient and stable adsorbents. In recent years, porous adsorbents with high surface area, adsorption capacity, and large pore volume have been a remarkable growth for the selective adsorption of cations and anions, organic compounds like dyes, aromatic hydrocarbons, and large organic molecules<sup>11</sup>.

Malachite Green (MG) is a methylated diamino-triphenylmethane dye that shows different colors in various pHs. The chemical properties of MG are

chemical formula:  $\text{C}_{23}\text{H}_{25}\text{N}_2\text{Cl}$ , molecular weight: 364.91 g/mol,  $\lambda_{\text{max}}$ : 618 nm. This substance is converted into cells to leucomalachite, a cytotoxic and carcinogenic pigment that can cause severe respiratory irritation. Mammals can be dangerously affected by 0.1  $\mu\text{g}$  of MG in their bodies<sup>12,13</sup>. It has been found that this substance causes liver cancer in mice and reproductive abnormalities in rabbits. Direct contact with MG can lead to DNA mutations<sup>12</sup>. Malachite green has been banned since 1983 in food-related applications. Nevertheless, using MG in the aquaculture industry as a fungicide agent and food additive for fish is very popular.

The utilization of mesoporous as an alternative adsorbent has many advantages, such as environmental friendliness, low cost, higher surface area, chemical stability, and a high potential for chemical modification<sup>14-16</sup>. Depending on the target pollutants, mesoporous can be used as an adsorbent both in natural or modified form. Among the various types of mesoporous, silica is the most utilized material consisting of a functionalized group. The overall

negative charge on the silica mesoporous by functionalized with organic materials is useful for the adsorption of cationic organic pollutants such as MG. According to the importance of this subject throughout the world, a new method with high adsorption capacity for removal of MG was investigated in this study. The objective of the research work was to assess the ability of acid-functionalized mesoporous for the removal of MG dye from an aqueous solution. The influence of contact time, initial concentration, and aqueous solution pH was estimated. The experimental adsorption results were analyzed by different adsorption isotherm and kinetic models.

### Materials and Methods

All reagents used were of analytical reagent-grade chemicals. The stock solution of the MG dye was prepared by dissolving the laboratory-grade of MG (Merck, Germany) in deionized water. Dimethylformamide (DMF), silica, 3-aminopropyltriethoxysilane, pure succinic acid, and ethanol 95% were used to synthesize and functionalize nanoporous silica. The FT-IR analysis was performed by an EQUINOX 55BRUKER, and the concentration of MG in solution was done with a UV-1600 Light Ray spectrophotometer. Nitrogen adsorption-desorption (BET) was used to determine the type of porosity, specific surface area, pore-volume, and diameter of SBA-15 by Belsorp Mini II porosimeter. The measurements were performed in 77 °K, and the sample was degassed at 300 °C. Mesopore volume and diameter are calculated by Barrett-Joyner-Halenda (BJH) pore size distribution curve. Average pore diameter and total pore volume are determined by Brunauer-Emmett-Teller (BET) curve.

#### Synthesis of nanoporous SBA-15

First, 60 g of surfactant of poly (ethylene glycol) P123 was weighed and added in the 1.7 L of 0.2 N hydrochloric acids into a 3-liter beaker. To get a uniform mixture, the solution was stirred for 15 h via a shaker. It was then poured into a 4-liter glass reactor, and the container was washed with 400 ml of deionized water. It was heated at a fixed

temperature of 40 °C for two h at a shaking speed of 53 RPM. Next, 127.5 g silica was added dropwise until it turned to a milky white after 20 min while the addition of silica was speeded up. The suspension was stirred at the same temperature for 24 h, continuously. After this time, the suspension was heated at the temperature of 100 °C for 48 h. Then, the residual was filtered and rinsed with water and ethanol. After drying, it was soxhlet with ethanol until all its surface surfactants were extracted. Then it was calcined in a furnace at the temperature of 600 °C for 6 h so that all surfactants oxidized and existed in the form of CO<sub>2</sub><sup>1</sup>.

#### Addition -COOH group

One gram of SBA-15 was dispersed in 25 ml of dry DMF. The amount of 0.2 g of succinic anhydride and 0.02 g of N,N<sub>0</sub>-dicyclohexylcarbodiimide (DCC) were separately prepared in the container containing 25 ml of DMF. Next, the solution containing SBA-15 was added dropwise into the solution containing succinic anhydride, which was well stirred on the shaker. After it, the solution was continuously stirred for 24 h. Then it was washed with DMF and ethanol, soxhlet with ethanol, and finally dried in the incubator<sup>17</sup>.

#### Adsorption process

The adsorption process was carried out by batch mode in various pH and initial concentrations of MG at contact times with the adsorbent dose of 20 mg at the lab temperature of 22 °C. After the adsorption process, the suspension was filtered, and the concentration of the remaining MG was measured by a UV spectrometer in the maximum wavelength of 618 nm. Then q<sub>e</sub> was calculated using the equation 1 as follow expression:

$$q = \frac{C_0 - C}{m} \times V \quad (1)$$

Where q is the adsorption capacity, C<sub>0</sub> and C<sub>e</sub> are the initial and equilibrium concentration of MG, V is the volume of the solution, and m is the amount of the adsorbent.

For a kinetic study of the adsorption process, 100 ml of a solution containing 30 mg.l<sup>-1</sup>

solution of MG was mixed with 20 mg of synthesized nanoporous as an adsorbent. The suspension was shaken at 125 RPM, and the sampling was done at contact times of 0 to 120 min. The samples were filtered, and the concentration of the remaining MG was

measured in each sample.

## Results

### Porosimetry analysis

The results from BET and BJH curves for SAB-15 and SAB-15-COOH are represented in table 1.

**Table 1:** Parameters obtained by BET and BJH for SAB-15 and the functionalized of SAB-15

Samples	Parameters			
	$S_{BET}$ ( $m^2 \cdot g^{-1}$ )	$V_{Nano}$ ( $cm^3 \cdot g^{-1}$ )	$V_{total}$ ( $cm^3 \cdot g^{-1}$ )	$D_{meso}$ (nm)
SBA-15	603	1.04	1.12	20.12
SBA-15-COOH	277	1.30	1.29	18.00

Nitrogen adsorption and desorption isotherm for calcined SBA-15 is depicted in figure 2a, and pore size distribution for calcined SBA-15 is depicted in figure 2b.

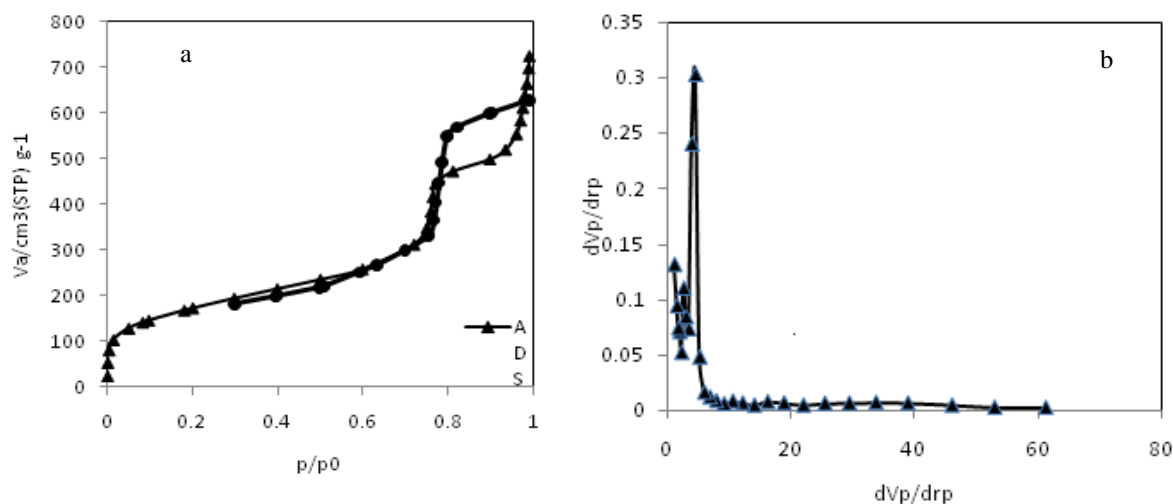


**Figure 2:** a) Nitrogen adsorption- desorption isotherm and b) pore size distribution for calcined SBA-15

Figures 3a and b show adsorption-desorption isotherm, and pore size distribution of the carboxylic agent on the surface of nanoporous. The

decrease in the surface area (from 603 to 277 nm) indicates the coupling of  $-COOH_2$  groups with functional groups on the pore surface of silica<sup>18</sup>.

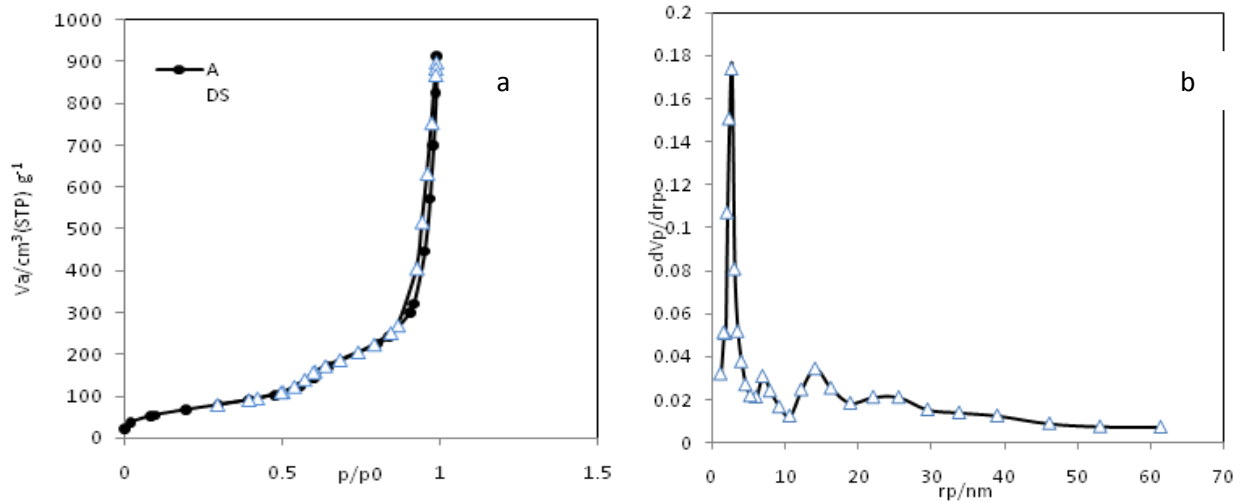


Figure 3: a: Nitrogen adsorption - desorption isotherm and b) pore size distribution for calcined SBA-15-COOH

**XRD Analysis**

Figure 4a shows the X-Ray Diffraction (XRD) pattern of SBA-15, and figure 4b shows for SBA-15-COOH. The peaks at  $2\theta = 1.72, 1.46, 0.84$  are related to crystal structures 110, 100, and 210, respectively.

**FT-IR analysis**

Figure 5 illustrates FT-IR spectra of the synthesized SBA-15 and functionalized material of SBA-15-COOH, which was scanned in the range of  $400-4000\text{ cm}^{-1}$ .

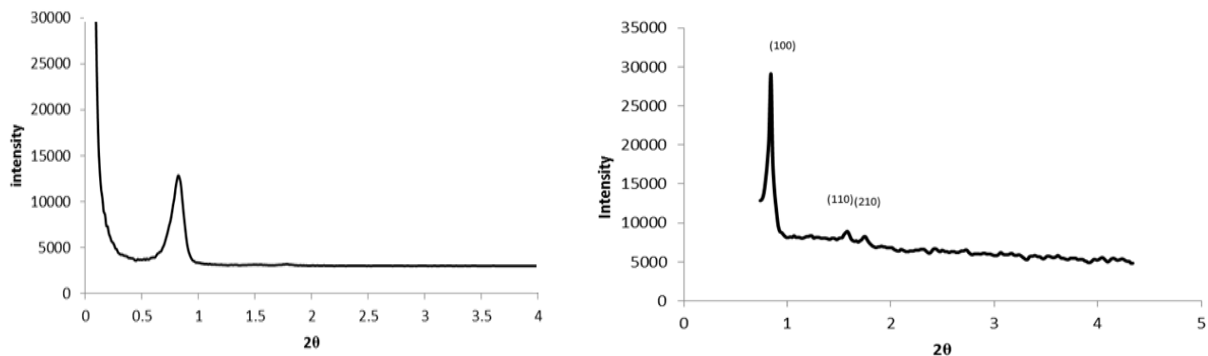


Figure 4: a. XRD spectra of SBA-15; and b. XRD spectra of SBA-15- COOH

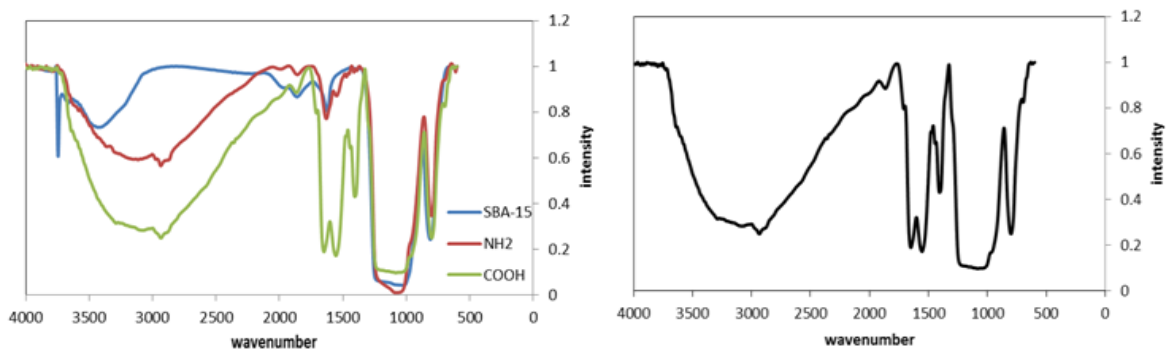
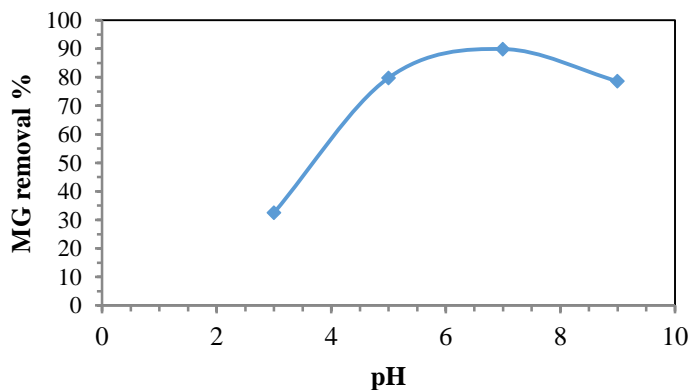


Figure 5: FT-IR spectra of SBA-15 and SBA-15-COOH

**Effect of pH on MG removal**

The experiments were conducted at 30 mg.l<sup>-1</sup> initial MG concentration with 20 mg adsorbent

mass at 120 min contact time. Figure 6 shows the effect of pH on the adsorption of MG by the synthesized nanoporous silica.



**Figure 6:** Effect of pH on MG removal by nanoporous functionalized silica

**Effect of contact time and initial concentration on adsorption removal**

In order to reach equilibration time for maximum uptake and to know the kinetics of the adsorption process, the adsorption of malachite green on acid-functionalized nanoporous silica adsorbent was studied as a function of contact time, and results are shown in figure 7.

According to figure 7, the time required for equilibrium adsorption was 60 min, and so the efficiency of the adsorbent for its use in wastewater treatment. Thus, the optimum equilibrium adsorption was chosen for one h. Also, the effect of C<sub>0</sub> on the adsorption capacity of MG by nanoporous adsorbent is shown in figure 7.

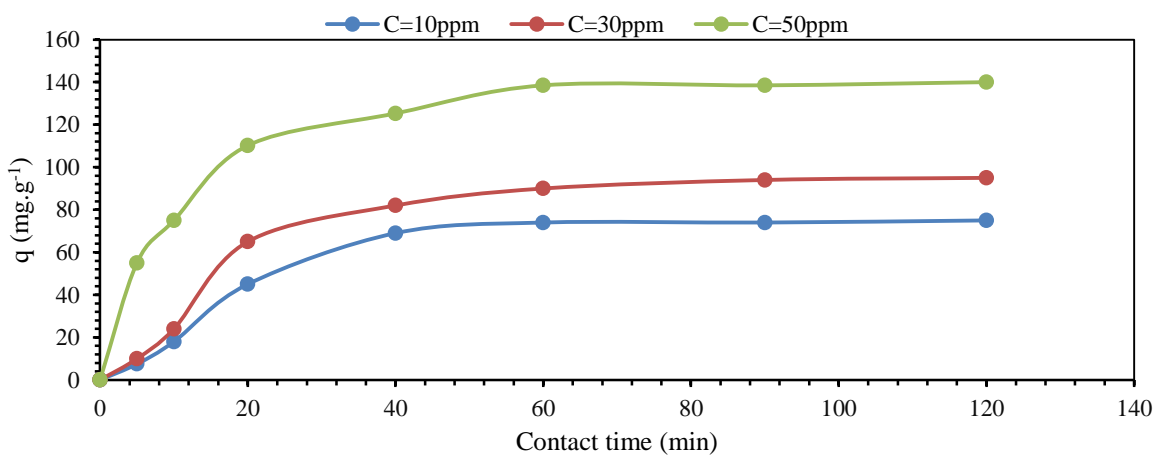


**Figure 7:** Effect of initial concentration and contact time on the adsorption capacity of MG by nanoporous silica at pH= 6.5



### Adsorption isotherm

The Freundlich isotherm applies to both monolayer and multilayer adsorption<sup>19</sup>. The linear form of the Freundlich equation is expressed as:

$$\log q_e = \log K_F + \frac{1}{n} \log C_e \quad (2)$$

The Langmuir isotherm assumes monolayer adsorption on a uniform surface with a finite

number of adsorption sites. The linear form of the Langmuir isotherm model is described as:

$$\frac{C_e}{q_e} = \frac{1}{K_L q_m} + \frac{C_e}{q_m} \quad (3)$$

The experimental data of the adsorption process were fitted by both Freundlich and Langmuir isotherms<sup>19</sup>. Table 2 depicts the calculated parameters according to the linearity of Freundlich and Langmuir isotherm models.

**Table 2:** Freundlich and Langmuir constants for the adsorption of MG onto synthesized nanoporous.

Isotherm	Langmuir			Freundlich		
	q <sub>m</sub> <sup>a</sup>	b <sup>b</sup>	R <sup>2</sup>	n	K <sub>F</sub> <sup>c</sup>	R <sup>2</sup>
Malachite green	116.3	0.719	0.8369	1.15	6.78	0.9954

a: mg.g<sup>-1</sup>, b: L.mg<sup>-1</sup> c: mg.g<sup>-1</sup>

### Adsorption kinetic

The adsorption kinetic equation is checked out as one of the system analysis methods. The pseudo-first and pseudo-second-order kinetic models are the most useful models to survey an adsorption system. After integrating with initial conditions (interval time of t = 0 to t = t and q = 0 to q = q<sub>e</sub>), the pseudo-first-order kinetics is presented in equation 4: (20)

$$\log(q_e - q_t) = \log q_e - \frac{k_1}{2.303} t \quad 4$$

The pseudo-second-order kinetic equation is based on this hypothesis that the rate of occupation sites is proportional to the square of the number of the occupied adsorption sites. After integrating

with the initial conditions, the linear equation can be written as equation 5:<sup>20</sup>

$$\frac{t}{q_t} = \frac{1}{k_2 q_e^2} + \frac{1}{q_e} t \quad 5$$

q<sub>e</sub> and q (mg.g<sup>-1</sup>) are the amounts of adsorption at the equilibrium and specified time, k<sub>1</sub> (min<sup>-1</sup>) is the rate constant of the first-order adsorption, and k<sub>2</sub> (g.mg<sup>-1</sup>.min<sup>-1</sup>) is the rate constant of the second-order adsorption. The data from the adsorption process were evaluated using two kinetics models of first and second-order equations. The models were obtained by drawing curves (t/q) and log(q<sub>e</sub>-q) via time (t). Table 3 represents the calculated data according to the pseudo-first and pseudo-second-order kinetic models.

**Table 3:** Pseudo - first order and second order constants for the adsorption of MG onto synthesized nanoporous.

Adsorbent	pseudo-first-order			pseudo-second-order		
	q <sub>e</sub> <sup>a</sup>	K <sub>1</sub> <sup>b</sup>	R <sup>2</sup>	q <sub>e</sub> <sup>a</sup>	K <sub>2</sub> <sup>c</sup>	R <sup>2</sup>
Malachite green	138.03	0.013	0.9689	90.09	3.159	0.8634

a:(mg.g<sup>-1</sup>), b: (min<sup>-1</sup>), c:(g.mg<sup>-1</sup>.min<sup>-1</sup>)

### Discussion

The high porosity of SBA-15 material indicates a high surface area of it (603 m<sup>2</sup>.g<sup>-1</sup>) that is due to the high porous surface, and it makes a very suitable adsorbent for MG adsorption. The average pore diameter of 20.12 nm is a suitable pore size to the entrance of the MG molecule as well as for the functional

groups which were seated in the pore area at the functionalizing step.

Nitrogen adsorption-desorption isotherms of synthesized and functionalized materials, according to IUPAC classification, are of type IV that confirms mesoporosity of this synthesized compound. The existence of an inverse loop between nitrogen adsorption-desorption on the

surface branches is a result of capillary condensation in the pores of the mesoporous silica arising from the liquefaction of the absorbed gas in the cylinder pores. Desorption is delayed (evaporation occurs at a lower partial pressure), which is one of the characteristics of mesoporous materials in type IV adsorption isotherm, and it was well observed that it is related to mesoporous materials. In SBA-15, this inverse loop is observable in the sorption isotherm diagram between the partial pressures of 0.7 and 0.9. Since the special form of each loop is identified with its special pore structure, in this isotherm, the inverse loop is of type  $H_1$ . The  $H_1$  loop is therefore indicative of uniform pores with narrow size distribution.

The comparison of the adsorption-desorption isotherms related to functionalize and unfunctionalized SBA-15, a decrease in the amount of inverse loop was noticed related to functionalize SBA-15, which was due to a decrease in capillary condensation and in the surface area of the filled pore. A comparison of the isotherms confirms the fact that a remarkable decrease in the amount of inverse loop caused the capillary condensation when an agent was seated on the surface. The sharp peak at  $2\theta = 0.84$  indicates a hexagonal structure with high order porosity(10). The weak peak of 100 results from the filling of the pores and decreasing pore order of the structure of SBA-15 which confirms the entrance of functional groups into the pores of the mesoporous.

The peaks between  $800$  and  $1100\text{ cm}^{-1}$  are related to bending vibration of condense silica Si-O-Si that are placed symmetrically. The  $1703\text{ cm}^{-1}$  peak, which is also relatively sharp, indicates the stretching vibration of the Si-O that shows the formation of the Si-O-Si bonds and verifies silica structure formation. The peaks that appeared in  $2890$  and  $2930\text{ cm}^{-1}$  are assigned to the stretching vibration of aliphatic carbons. The peak at  $1459\text{ cm}^{-1}$  is related to the bending vibration of aliphatic carbons, and the highest peak at  $1629\text{ cm}^{-1}$  is assigned to bending vibration  $-\text{COOH}$ . The appeared peaks in the ranges from  $1600$  to  $1800\text{ cm}^{-1}$  are related to bending vibration of the double

bonds of carbon-oxygen. The stretching vibration of OH is over  $3000\text{ cm}^{-1}$  that cannot be viewed due to water<sup>21</sup>. This information and compare the peaks confirm the presence of functional groups on the surface.

According to figure 6, MG adsorption was favorable at  $\text{pH} > 6.5$ . The decrease in the adsorption at low pHs may be attributed to increase in the number of positively charged surface sites. Also, the lower adsorption of MG at acidic pH is due to the excess  $\text{H}^+$  ions competing with MG cations toward the adsorption active sites of nanoporous silica. When the pH of the system increased, the number of negatively charged surface sites increased, which is favor the adsorption of positively charged MG molecules due to columbic interaction.

The contact time between adsorbent and adsorbate species plays a main role in the adsorption of pollutants from wastewater and contaminated water by adsorption at a specific pH. Figure 7 indicates that the rate of adsorption is rapid in the initial steps and becomes slow in later steps up to saturation is achieved. This is clear that a large number of surface active sites are available for MG adsorption at the initial stages, and after this time, the unoccupied surface sites are difficult to be occupied due to repulsion force between the molecules on the adsorbate and in the bulk phases<sup>22</sup>.

From figure 7, it is obvious that the amount of MG adsorption capacity decreased with the increase in initial concentration. Also, it was found that the equilibrium time, as well as time required to achieve a fraction of adsorption, is independent of initial MG concentration.

The high regression coefficient ( $R^2 = 0.99$ ) revealed the adsorption process was well fitted by Freundlich isotherm model. The adsorbent in the removal of MG had a high adsorption capacity equal to  $116.3\text{ mg.g}^{-1}$ . This shows that the adsorption of MG takes place on multilayer porous materials. The multilayer adsorption can be related to the kind of adsorption of MG in the pores. It is probable that MG molecules are blocked by the molecules which were adsorbed onto the surface of pores.



The pseudo-first and second-order models were utilized to illustrate the adsorption rate. The pseudo-first-order model is based on the assumption that the rate of MG adsorption increases proportionally with the quantity of MG adsorbed from the bulk solution. The regression coefficient for the pseudo-first-order model is slightly higher than that of the pseudo-second-order model so, it is acceptable. This denoted that the overall adsorption rate is controlled by the slowest step, also known as the rate-limiting step. In these cases, the adsorption rate is influenced by several steps. From table 3, pseudo-second-order is also applicable in describing the rate of MG adsorption onto acid-functionalized nanoporous. Similar findings were reported by Banerjee and Sharma<sup>23</sup> for MG adsorption. The rate constant,  $k_2$  was  $3.159 \text{ mg.g}^{-1}.\text{min}^{-1}$ . Based on the Arrhenius equation, a high  $k_2$  represents a more spontaneous reaction caused by the lower activation energy.

The high  $R^2$  showed that a better agreement with pseudo-first-order models, and this demonstrates that adsorption of MG on the nanoporous silica is related to initial MG concentration. The decreasing of the surface is not very noticeable with the addition of the MG onto the functionalized surface. This is because of the exclusive interaction of the molecules MG with the functional group.

### Conclusion

In this research, the nanoporous adsorbent, SBA-15, was synthesized by hydrothermal method, and next, the COOH group was placed on the adsorbent by post-synthesis method. The structure was identified using BET, XRD, and IR. The application of adsorbent was carried out by batch mode for removal of MG. The obtained results indicate that the multilayer was happening in the adsorption of MG on the surface of functionalized nanoporous. The high surface area of the functionalized nanoporous silica makes it a very good adsorbent. Therefore, this adsorbent can use in the treatment of wastewaters and basic polluted water.

### Acknowledgments

We thank the staff of the instrumental analysis laboratory for help.

### Funding

This research was funded by the department of chemistry.

### Conflict of interest

The authors declare no conflict of interest.

This is an Open-Access article distributed in accordance with the terms of the Creative Commons Attribution (CC BY 4.0) license, which permits others to distribute, remix, adapt, and build upon this work for commercial use.

### References

1. Trewyn BG, Slowing II, Giri Set, et al. Synthesis and functionalization of a mesoporous silica nanoparticle based on the sol-gel process and applications in controlled release. *Acc Chem Res.* 2007;40(9):846-53.
2. Ozin GA, Cademartiri L. Nanochemistry: what is next. *Small.* 2009;5(11):1240-4.
3. Taguchi A, Schüth F. Ordered mesoporous materials in catalysis. *Microporous Mesoporous Mater.* 2005;77(1):1-45.
4. Huo Q, Margolese DI, Ciesla U, et al. Organization of organic molecules with inorganic molecular species into nanocomposite biphasic arrays. *Chemistry of Materials.* 1994;6(8):1176-91.
5. Radu DR, Lai CY, Wiench JW, et al. Gatekeeping layer effect: A poly (lactic acid)-coated mesoporous silica nanosphere-based fluorescence probe for detection of amino-containing neurotransmitters. *Journal of the American Chemical Society.* 2004;126(6):1640-1.
6. Katiyar A, Yadav S, Smirniotis PG, et al. Synthesis of ordered large pore SBA-15 spherical particles for adsorption of biomolecules. *J Chromatogr A.* 2006;1122(1-2):13-20.
7. Juang LC, Wang CC, Lee CK. Adsorption of basic dyes onto MCM-41. *Chemosphere.* 2006;64(11):1920-8.

8. Salmani M, Zarei S, Ehrampoush M, et al. Evaluations of pH and high ionic strength solution effect in cadmium removal by zinc oxide nanoparticles. *Bioresour Technol.* 2013;17(4): 583-93.
9. Crini G. Non-conventional low-cost adsorbents for dye removal: a review. *Bioresour Technol.* 2006;97(9):1061-85.
10. Zheng-fei MA, Xiao-qin LIU, Hu-qing YAO, et al. Advances in adsorption principles and adsorption processes. *J Nanjing Univ Technol.* 2006;1:1-5.
11. Lam KF, Ho KY, Yeung KL, et al. Selective adsorbents from chemically modified ordered mesoporous silica. *Studies in Surface Science and Catalysis.* 2004; 154, Part C: 2981-86.
12. Culp S, Beland F, Heflich R, et al. Mutagenicity and carcinogenicity in relation to DNA adduct formation in rats fed leucomalachite green. *Mutat Res.* 2002;506:55-63.
13. Srivastava S, Sinha R, Roy D. Toxicological effects of malachite green. *Aquat Toxicol.* 2004;66(3):319-29.
14. Thahir R, Wahab AW, La Nafie N, et al. Synthesis of high surface area mesoporous silica SBA-15 by adjusting hydrothermal treatment time and the amount of polyvinyl alcohol. *Open Chem.* 2019;17(1):963-71.
15. Qu W, Yuan T, Yin G, et al. Effect of properties of activated carbon on malachite green adsorption. *Fuel.* 2019;249:45-53.
16. Cashin VB, Eldridge DS, Yu A, et al. Surface functionalization and manipulation of mesoporous silica adsorbents for improved removal of pollutants: a review. *Environ Sci (Camb).* 2018;4(2):110-28.
17. Shah SM, Makhdoom AR, Su X, et al. Synthesis of sulphonic acid functionalized magnetic mesoporous silica for Cu(II) and Co(II) adsorption. *Microchem J.* 2019;151:104194.
18. Sonwane C, Bhatia S. Characterization of pore size distributions of mesoporous materials from adsorption isotherms. *J Phys Chem B.* 2000;104(39):9099-110.
19. Ahmad MA, Alrozi R. Removal of malachite green dye from aqueous solution using rambutan peel-based activated carbon: Equilibrium, kinetic and thermodynamic studies. *J Chem Eng.* 2011;171(2):510-6.
20. Largitte L, Pasquier R. A review of the kinetics adsorption models and their application to the adsorption of lead by an activated carbon. *Chem Eng Res Des.* 2016;109:495-504.
21. Popova MD, Szegedi Á, Kolev IN, et al. Carboxylic modified spherical mesoporous silicas as drug delivery carriers. *Int J Pharm.* 2012;436(1-2):778-85.
22. Wang H, Yuan X, Zeng G, et al. Removal of malachite green dye from wastewater by different organic acid-modified natural adsorbent: kinetics, equilibriums, mechanisms, practical application, and disposal of dye-loaded adsorbent. *Environ Sci Pollut Res.* 2014;21(19):11552-64.
23. Banerjee S, Sharma YC. Equilibrium and kinetic studies for removal of malachite green from aqueous solution by a low cost activated carbon. *J Ind Eng Chem.* 2013;19(4):1099-105.